Solitary excitations in B-Z DNA transition: A theoretical and numerical study

Wilber Lim*

Department of Physics, Faculty of Science, National University of Singapore, 2 Science Drive 3, Singapore 117542, Singapore

(Received 12 November 2006; published 30 March 2007)

The molecular mechanism of B-Z DNA transition remains elusive since the elucidation of the left-handed Z-DNA structure using atomic resolution crystallographic study. Numerous proposals for the molecular mechanism have been advanced, but none has provided a satisfactory explanation for the process. A nonlinear DNA model is proposed which enables one to derive various hypothesized molecular mechanisms, namely the Harvey model, Zang and Olson model, and the stretched intermediate model, by imposing certain constraints and conditions on the model. These constraints raise the need to reevaluate experimental investigations on B-Z DNA transition.

DOI: 10.1103/PhysRevE.75.031918 PACS number(s): 87.14.Gg, 05.45.Yv, 87.15.He, 05.10.−a

I. INTRODUCTION

The possibility that nonlinear solitary excitations may play an important role in phenomenon such as deoxyribonucleic acid (DNA) transcription, replication, denaturation and conformational transitions has attracted the considerable attention of both theoreticians and experimentalists [1–9]. However, the application of the nonlinear physics of DNA to the conformational transition from the right-handed B-DNA helix to the left-handed Z-DNA helix is somewhat rather reserved. Such reservation arises mainly due to the difficulty in selecting the dominant motions involved in B-Z DNA transition as experimental results are often controversial and inconclusive [10–13]. For instance, nuclear magnetic resonance (NMR) experiments on B-Z DNA transition suggest that hydrogen bonds between nucleobases remain intact throughout the transition whereas melting experiments suggest otherwise, leading to two contrasting molecular mechanisms—the Harvey model [14], in which no hydrogen bonds are broken and base flipping is facilitated by longitudinal breathing modes, and the Wang model, which involves base pair opening before rotation about the glycosyl bond [15]. Such contradictions prevent one from painting an accurate dynamical picture of the B-Z DNA transition. Despite these shortcomings, several attempts have been made to describe solitary excitations in B-Z DNA transition. Jensen *et al.* have shown using a rod-like DNA model that soliton waves exist for the propagation of B-Z junction during the transition [16]. Their model however does not describe in detail how base flipping is achieved in this process. On the other hand, Zang and Olson adopted the Wang model and showed that base extrusion and flipping can be described numerically as solitary excitations [17]. Nevertheless, they predicted the existence of Hoogsteen base pairs in the transition which have not observed experimentally. Furthermore, the obtained solitary wave solution is based on a particular molecular mechanism. More recently however, atomistic simulations of a short oligomer undergoing B-Z DNA transition have shown that the oligomer unwinds and stretches during the transition and the rotation of the base about its glycosyl bond can be described using a solitary wave [18–21]. The advantage of this atomistic simulation is that no prior assumption regarding the molecular mechanism is made. Its main disadvantage, however, is that this holds only for a short oligomer.

The objective of this paper is twofold, to construct a general model of DNA that can describe B-Z DNA transition without invoking and assuming any specific molecular mechanism as well as to show that by varying certain parameters in the nonlinear model, different molecular mechanisms can be derived, namely the Harvey model, the Zang-Olson and Wang model as well as the stretched intermediate model.

II. DNA HAMILTONIAN

The model Hamiltonian that is constructed is essentially based on previous models developed by Yomosa, Zang, and Olson as well as Volkov [2,22]. These models were successful in describing open states in DNA as well as DNA conformational transitions such as B-A DNA transition. Three conformational variables are selected to describe the transition—glycosydic bond angle χ, longitudinal displacement of the nucleotide r, and base extrusion angle ϕ, as they are common to all the molecular mechanisms proposed so far. Any inhomogeneities and conformational changes in the sugar-pucker ring are ignored in the present analysis. This leads us to propose the following model

$$H = T + V_1 + V_2 + V_{\text{interstrand}}, \tag{1}$$

where T is the kinetic energy term,

$$T = \sum_n \left(\frac{1}{2}\mu \dot{r}_n^2 + \frac{1}{2} J \dot{\chi}_{n^2} + \frac{1}{2} I \dot{\phi}_{n^2} \right) \tag{2}$$

and V_1 is the intrastrand potential energy of a single polynucleotide strand

$$V_1 = \sum_n \frac{1}{2} \exp(\lambda_1 r_0)\{\exp\{-\lambda_1 \sqrt{r_n^2 + 2b^2[1-\cos(\phi_{n+1}-\phi_n)]}\} + \exp\{-\lambda_1 \sqrt{r_{n-1}^2 + 2b^2[1-\cos(\phi_n - \phi_{n-1})]}\}\} \times A_n[1-\cos(2\chi_n)] + \sum_n \exp(\lambda_2 r_0)$$

*Electronic address: wilber.lim@aya.yale.edu

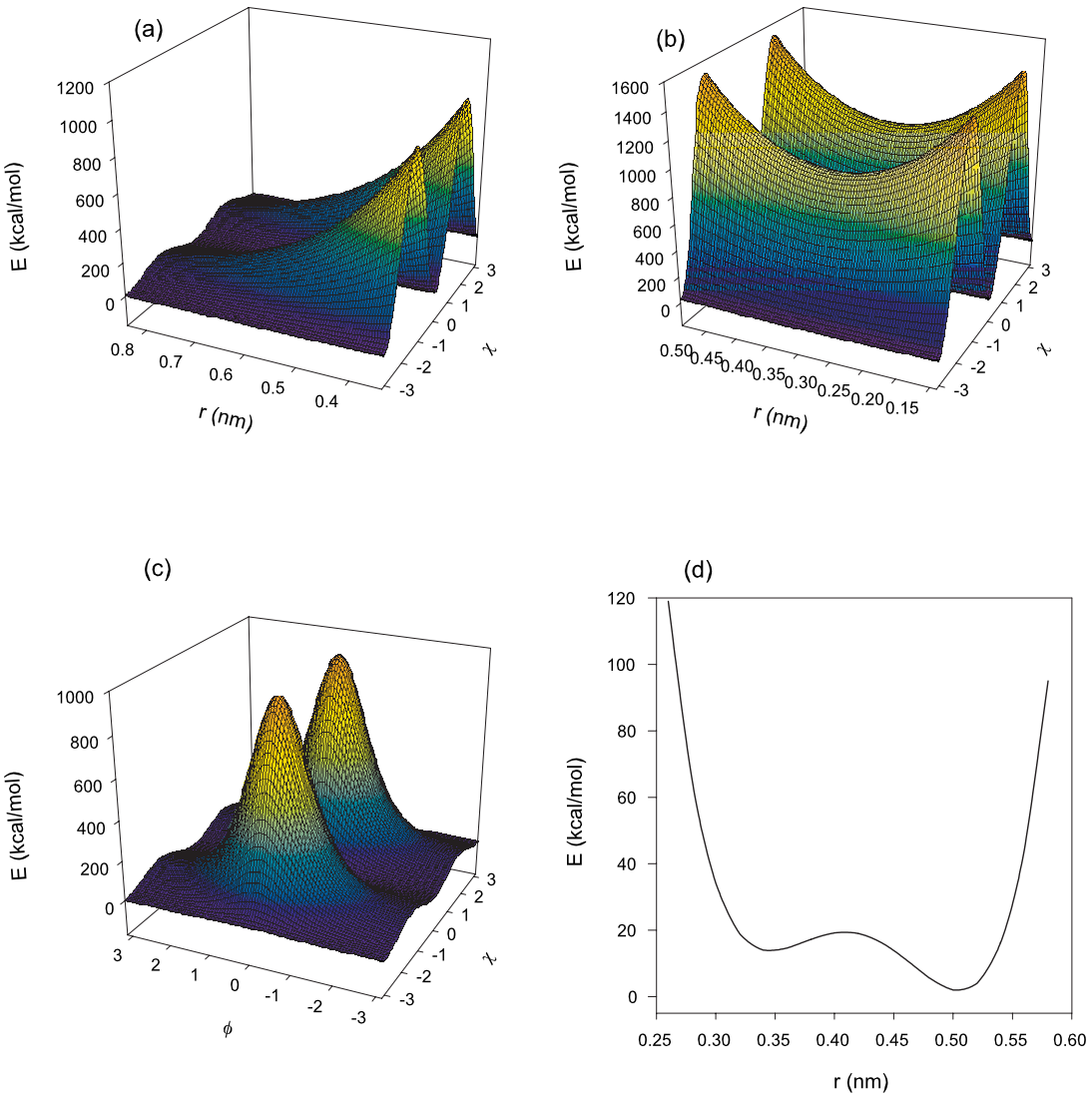

FIG. 1. (Color online) Plots of various potential energy terms in the DNA model. (a) Variation of glycosidic torsion energy with longitudinal displacement r for a nucleobase at either end of the polynucleotide strand. (b) Variation of glycosidic torsion energy with longitudinal displacement r for a nucleobase in the presence of two adjacent nucleobases. (c) Variation of glycosidic torsion energy with ϕ for a nucleobase at either end of the polynucleotide strand. (d) Volkov double well potential. The wells correspond to B-DNA state (at $r=0.34$ nm) and S-DNA state (at $r=0.50$ nm). Height of the barrier ≈ 9 kcal/mol. Parameters used are $d=0.42$ nm, $a=0.08$ nm, $\epsilon_0=8$ kcal/mol, $\epsilon_1=-6$ kcal/mol, and $\epsilon=11$ kcal/mol.

$$\times \exp\{-\lambda_2\sqrt{r_n^2 + 2b^2[1-\cos(\phi_{n+1}-\phi_n)]}\}$$
$$\times K_n[1-\cos(\chi_{n+1}-\chi_n)]$$
$$+\sum_n \{H_n[1-\cos(\phi_n)] + S_n[1-\cos(\phi_n-\phi_{n-1})]\}$$
$$+\sum_n \left[\epsilon_0 + \epsilon_1\left(\frac{(r_n-d)}{a}\right) + \epsilon\left(1-\frac{(r_n-d)^2}{a^2}\right)^2\right]. \quad (3)$$

In Eq. (3), A_n corresponds to the electrostatic repulsion that bases experience as they rotate about the glycosyl bond in their canonical positions. Such repulsion can be reduced simply by stretching the helix or via base pair opening as indicated in Fig. 1. In terms of $\{\chi, r, \phi\}$, B-DNA is denoted by $\{0, 0.34, 0\}$ while Z-DNA is represented by $\{\pi, 0.373, 0\}$. V_2 is the interstrand potential energy of the complementary strand similar in form except quantities are primed. Each nucleotide pair is assumed to rotate about the glycosyl linkage in unison and relative longitudinal displacement within each nucleotide pair is neglected. Interstrand potential is thus given by

$$V_{\text{interstrand}} = \sum_n B_n[1-\cos(\phi_n)\cos(\phi_n')]. \quad (4)$$

Note that coupling between extrusion and longitudinal displacement is ignored. In the continuum approximation, the Lagrangian corresponding to Eqs. (1)–(4) can be written as follows:

$$L = \int \frac{dz}{r_0}\frac{1}{2}\mu\dot{y}^2 + \frac{1}{2}J\dot{\chi}^2 + \frac{1}{2}I\dot{\phi}^2 - \frac{1}{2}\left\{\exp\left\{\lambda\left[r_0 - \sqrt{(r_0+y)^2 + b^2 r_0^2\left(\frac{\partial\phi}{\partial z}\right)^2}\right]\right\} + \exp\left\{\lambda\left[r_0 - \sqrt{(r_0-y)^2 + b^2 r_0^2\left(\frac{\partial\phi}{\partial z}\right)^2}\right]\right\}\right\}$$
$$\times\left\{A[1-\cos(2\chi)] + Kr_0^2\left(\frac{\partial\chi}{\partial z}\right)^2\right\} - H[1-\cos(\phi)] - \frac{Sr_0^2}{2}\left(\frac{\partial\phi}{\partial z}\right)^2 - V_2(\chi',\phi',y') - B[1-\cos(\phi)\cos(\phi')]$$
$$- 2\epsilon_0 - 2\frac{\epsilon_1 r_0}{a} - \epsilon\left\{\left[1 - \frac{(r_0+y-d)^2}{a^2}\right]^2 + \left[1 - \frac{(r_0-y-d)^2}{a^2}\right]^2\right\}. \quad (5)$$

III. PARAMETERS

Parameters are obtained from existing experimental and computational results. The mass of a G-C nucleotide pair $2M$ is taken to be 615 g/mol [23]. By treating a base pair as a thin circular disk with radius $R=0.5$ nm, the moment of inertia about the glycosyl linkage is $J=\frac{1}{4}MR^2$. I is the moment of inertia of a nucleotide about an axis parallel to the helical axis and is taken to be Mb^2 where $b=0.4$ nm. For all practical purposes, the attenuation factor $\lambda_1,\lambda_2=\lambda=5$ nm^{-1} since molecular packing becomes negligible beyond a distance of 1 nm [24,25], or approximately the diameter of a base pair $2R$. When molecular packing is negligible, the energy profiles obtained from variation of the torsion angle about the glycosyl linkage corresponds to the intrinsic energetics of the glycosyl torsion. Consequently, $A_n=A_0\exp(2\lambda R)$ where $A_0 \approx 10.0$ kcal/mol for guanine and $A_0 \approx 15$ kcal/mol for cytosine [26,27]. Note, however, that in the forthcoming numerical and theoretical analysis, the difference in A_n for the bases is ignored. K_n is determined from the stacking energy of the base pairs [49], which is approximately 11.95 kcal/mol [28,29]. ϵ_0, d, a, and ϵ_1 in the Volkov double well potential term are determined such that the wells correspond to the B-DNA state and the S-DNA state [30,31]. The potential energy increases sharply for $r>0.55$ nm due to the strong covalent bonds and $r<0.30$ nm as a result of electrostatic repulsion [32]. ϵ, on the other hand, dictates the height of the barrier that has to be crossed between the B-DNA and S-DNA state which is known to be approximately 5–10 kcal/mol since the increase in stacking energy is partly compensated by a reduction in backbone energy [33,34]. S_n, H_n, and B_n are obtained from the experimental data of Nakanishi and Tsuiboi and Teitelbaum and Englander. Following Yomosa [2], by assuming $H_n=H$, $B_n=B$ and $2(H+B)\approx 4S$, we have $S\approx 0.69$ kcal/mol and $H=B \approx 0.69$ kcal/mol.

IV. HARVEY AND ZIPPER MODELS

The Harvey model is characterized by the following steps (1) Opening of a local cavity. (2) Base flipping within that cavity without any hydrogen bond breakage. (3) Propagation of the cavity. The zipper model, on the other hand, generalizes the propagation process to that of a B-Z junction without describing in detail the structure of the junction. These steps can be mathematically derived from Eq. (5) by assuming that the time averaged value of ϕ is zero, i.e., $\phi=\langle\phi\rangle=0$. With that, the Euler-Lagrange equations for Eq. (5) are simplified to

$$\mu\ddot{y} + A\lambda\sinh(\lambda y)[1-\cos(2\chi)] + \lambda Kr_0^2\sinh(\lambda y)\times\left(\frac{d\chi}{dz}\right)^2 + \frac{\epsilon}{a^2}\left[\frac{24(r_0-d)^2}{a^2} - 8\right]y = 0, \quad (6)$$

$$\mu\ddot{y}' + A\lambda\sinh(\lambda y')[1-\cos(2\chi)] + \lambda Kr_0^2\sinh(\lambda y')\times\left(\frac{d\chi}{dz}\right)^2 + \frac{\epsilon}{a^2}\left[\frac{24(r_0-d)^2}{a^2} - 8\right]y' = 0, \quad (7)$$

and

$$J\ddot{\chi} + 2A\cosh(\lambda y)\sin(2\chi) - 2Kr_0^2\cosh(\lambda y)\frac{d^2\chi}{dz^2} = 0. \quad (8)$$

Soliton solutions for χ can be obtained by considering the limit of small λy such that $\sinh(\lambda y)\to\lambda y$ and $\cosh(\lambda y)\to 1$. Under such conditions, together with the assumption $y=y'$, Eqs. (6)–(8) are reduced to

$$\mu\ddot{y} = -\Omega^2(z,t)y \quad (9)$$

and

$$J\ddot{\chi} + 2A\sin(2\chi) - 2Kr_0^2\frac{d^2\chi}{dz^2} = 0, \quad (10)$$

where $\Omega(z,t)$ is given by

$$\Omega^2(z,t) = \lambda^2\left\{A[1-\cos(2\chi)] + Kr_0^2\left(\frac{d\chi}{dz}\right)^2\right\} + \frac{\epsilon}{a^2}\left[\frac{24(r_0-d)^2}{a^2} - 8\right]. \quad (11)$$

After making the transformation $T=\sqrt{(4A/J)}t$ and $\xi=\sqrt{(2A/Kr_0^2)}z$, the solution to Eq. (10) is simply

$$\chi = \Phi(\xi-\xi_0-vT) = 2\arctan\{\pm\exp[\gamma(\xi-\xi_0-vT)]\}, \quad (12)$$

where $\gamma=(1-v^2)^{-1/2}$ and v is the soliton velocity. Inserting Eq. (12) into Eq. (11) gives

$$\Omega^2 = w^2\,\mathrm{sech}^2[\gamma(\xi-\xi_0-vT)] + \omega_0^2, \quad (13)$$

where $\omega_0^2=(\epsilon/a^2)[24(r_0-d)^2/a^2-8]$ and $w^2=2A\lambda^2(1+\gamma^2)$. For the time-dependent harmonic oscillator given by Eq. (9) and Eq. (13), if $\Omega(t)$ varies monotonically in an interval Δ

centered at time t_s that is much smaller than ω_0, then approximate analytical solutions can be expressed in the following form [35]:

$$y(t) = g(t)e^{i\gamma(t)} = a(t)e^{is(t)+i\theta} + b(t)e^{-is(t)+i\theta}, \tag{14}$$

where $a(t)$ and $b(t)$ are given by

$$a(t) = \frac{1}{2}a_1\left(1 + \frac{\omega_0}{\sqrt{w^2\,\mathrm{sech}^2[\gamma(\xi-\xi_0-vT)]+\omega_0^2}}\right), \tag{15}$$

$$b(t) = \frac{1}{2}a_1\left(1 - \frac{\omega_0}{\sqrt{w^2\,\mathrm{sech}^2[\gamma(\xi-\xi_0-vT)]+\omega_0^2}}\right), \tag{16}$$

and $s(t)$ is given by

$$\begin{aligned} s(t) &= \int_{t_s}^{t}\Omega(t')dt' \\ &= \frac{-1}{v\gamma}\sqrt{\frac{J}{4A}}\Bigg[\cosh[\gamma(\xi-\xi_0-vT)] \\ &\times\sqrt{\frac{2w^2\,\mathrm{sech}^2[\gamma(\xi-\xi_0-vT)]+2\omega_0^2}{2w^2+\omega_0^2+\omega_0^2\cosh[2\gamma(\xi-\xi_0-vT)]}} \\ &\times\Bigg\{\omega_0\sinh^{-1}\left(\sqrt{\frac{\omega_0^2\sinh^2[\gamma(\xi-\xi_0-vT)]}{w^2+\omega_0^2}}\right)+w \\ &\times\tan^{-1}\left(\sqrt{\frac{2w^2\sinh^2[\gamma(\xi-\xi_0-vT)]}{2w^2+\omega_0^2+\omega_0^2\cosh[2\gamma(\xi-\xi_0-vT)]}}\right)\Bigg\}\Bigg]_{t_s}^{t}. \end{aligned} \tag{17}$$

The amplitude and phase of $y(t)$ are thus given respectively by

$$g(t) = \sqrt{a^2(t)+b^2(t)+2a(t)b(t)\cos[2s(t)]}, \tag{18}$$

$$\gamma(t) = \tan^{-1}\left\{\frac{a(t)-b(t)}{a(t)+b(t)}\tan[s(t)]\right\}+\theta. \tag{19}$$

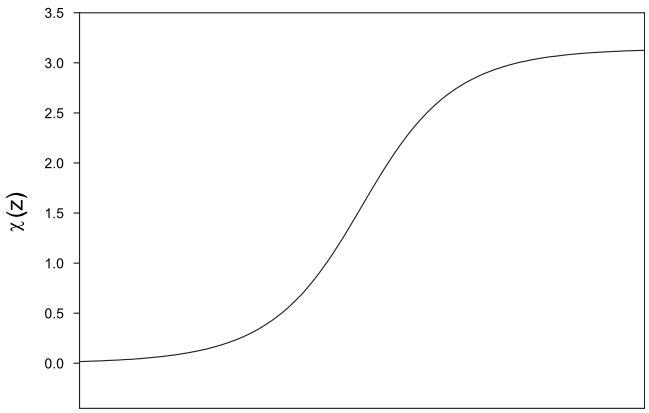

FIG. 2. Plot of Eq. (12). Base flipping of π in B-Z DNA transition is achieved via solitary excitations.

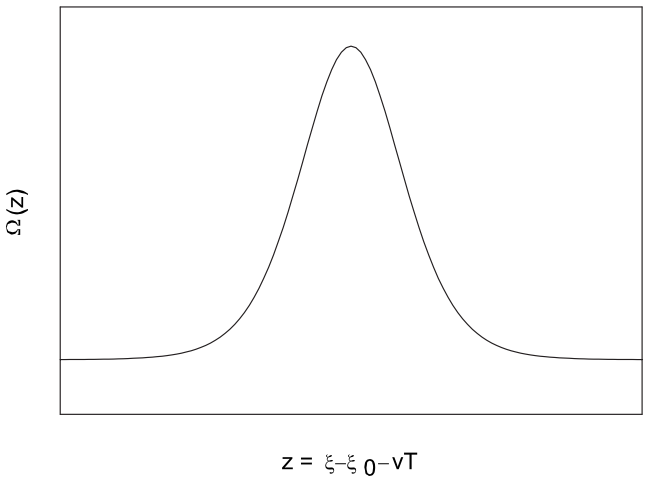

FIG. 3. Plot of time-dependent frequency for arbitrarily defined parameters. Maximum value of $\Omega(z)$ is given by $\sqrt{w^2+\omega_0^2}$ while minimum value is given by ω_0.

$\chi(t)$, $\Omega(t)$, and $g(t)$ are respectively plotted in Figs. 2–4. One can see that the amplitude for longitudinal displacement varies along the DNA strand to accommodate for base flipping, with the greatest variation at the point where χ changes the most. Similar to the local cavity in the Harvey model, the "wave packet" of amplitude oscillation travels along the strand together with the χ soliton.

V. ZANG-OLSON AND WANG MODEL

Unlike the Harvey model, the Zang-Olson and Wang model dictates that base flipping should occur after the base is rotated out of the helix. This can be seen in the present model if we make the following approximations: $y \ll r_0$ and $b \ll r_0$. These conditions can be achieved when the rise of the helix is enhanced by certain B-Z inducers, intercalating agents, unwrapping nucleosomes or mechanical stretching [36]. With that, the modifier for glycosidic potential terms becomes

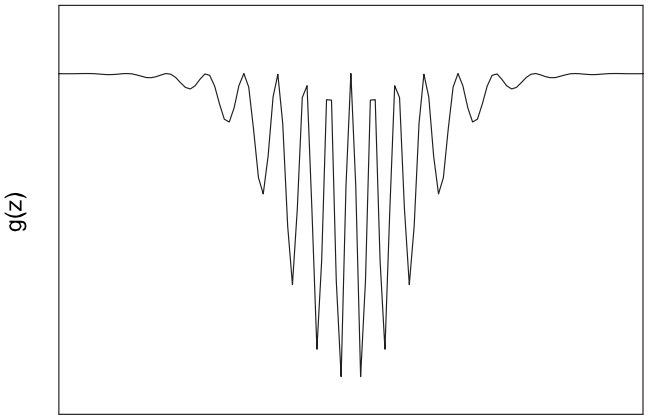

FIG. 4. Plot of longitudinal oscillation amplitude for arbitrary defined parameters.

$$\exp(\lambda r_0)\{\exp\{-\lambda\sqrt{r_n^2+2b^2[1-\cos(\phi_{n+1}-\phi_n)]}\}\}$$
$$\approx 1-\lambda r_0\left(\frac{b}{r_0}\right)^2+\lambda r_0\left(\frac{b}{r_0}\right)^2\cos(\phi_{n+1}-\phi_n)$$
$$=\alpha+\beta\cos(\phi_{n+1}-\phi_n). \quad (20)$$

The functional form of the modifier in Eq. (20) is similar to the modifier $[1+\cos(\phi)]$ Zang and Olson used in their model with the exception that relative displacement of the nucleobases are taken into account within the current model and the minimum of the modifier is $1-2\lambda r_0(b/r_0)^2$ instead of zero. Here, we can attempt to derive some interesting theoretical results based on Eq. (20). In the continuum approximation, the set of relevant Euler-Lagrange equations becomes

$$J\ddot{\chi}+2A\left[1-\lambda r_0 b^2\left(\frac{d\phi}{dz}\right)^2\right]\sin(2\chi)$$
$$-\left[1-\lambda r_0 b^2\left(\frac{d\phi}{dz}\right)^2\right]Kr_0^2\frac{d^2\chi}{dz^2}=0, \quad (21)$$

$$I\ddot{\phi}+\left\{2\lambda r_0 b^2 A[1-\cos(2\chi)]+\lambda b^2 K r_0^3\left(\frac{d\chi}{dz}\right)^2-Sr_0^2\right\}$$
$$\times\left(\frac{d^2\phi}{dz^2}\right)+H\sin(\phi)+B\sin(\phi)\cos(\phi')=0, \quad (22)$$

$$I\ddot{\phi}'+\left\{2\lambda r_0 b^2 A[1-\cos(2\chi)]+\lambda b^2 K r_0^3\left(\frac{d\chi}{dz}\right)^2-Sr_0^2\right\}$$
$$\times\left(\frac{d^2\phi'}{dz^2}\right)+H\sin(\phi')+B\sin(\phi')\cos(\phi)=0. \quad (23)$$

General analytical solutions to this set of coupled differential equations have not been found, but several particular solutions of interest can be obtained:

$$\phi=n\pi, \quad \phi'=m\pi, \quad \chi=\Phi(\xi-\xi_0-vT), \quad (24)$$

$$\phi=n\frac{\pi}{2}, \quad \phi'=m\frac{\pi}{2}, \quad \chi=\Phi(\xi-\xi_0-vT), \quad (25)$$

where $n-m=0,\pm1,\pm2,\ldots$. With the exception of solutions involving ϕ and ϕ' both being 0 or multiples of 2π, other solutions represent open states in which base flipping can occur. Other solutions of interest can be derived if certain approximations are made. For instance, if λ is very small, then in essence, motion about the glycosyl bond is decoupled from base pair opening. Equation (21) is thereby reduced to Eq. (10) whose solution is given by Eq. (12). Equations (22) and (23) are also simplified to

$$I\ddot{\phi}-Sr_0^2\left(\frac{d^2\phi}{dz^2}\right)+H\sin(\phi)+B\sin(\phi)\cos(\phi'), \quad (26)$$

$$I\ddot{\phi}'-Sr_0^2\left(\frac{d^2\phi'}{dz^2}\right)+H\sin(\phi')+B\sin(\phi')\cos(\phi), \quad (27)$$

whose solutions are explored in detail by Yomosa [2].

VI. STRETCHED INTERMEDIATE MODEL

We seek to obtain a numerical solution that resembles the stretched intermediate model obtained from atomistic simulations. Approximate solutions can be obtained by minimizing the following quantity using metropolis Monte Carlo–simulated annealing:

$$S_{\mathrm{SDET}}=\Delta t\sum_i\left(\frac{\vec{Y}_{i+1}+\vec{Y}_{i-1}-2\vec{Y}_i}{\Delta t^2}+\left.\frac{dU}{d\vec{Y}}\right|_{\vec{Y}=\vec{Y}_{i-1}}\right)^2. \quad (28)$$

"SDET" is the abbreviation for "stochastic difference equation with respect to time" [37]. The optimization protocol is as follows: Temperature T is reduced to $(1-\alpha_{\mathrm{sa}})T$ every K_{sa} steps starting from an initial temperature T_{i} to a final temperature of T_{f}. $\Delta t=19.802$ ps. Number of base pairs N is six and the total number of annealing steps employed is 1.0×10^7. For the given size of the oligomer, the total time of simulation T_{total} is 2.0 ns. Various simulated annealing schemes were adopted and the results are qualitatively similar to the atomistic simulations and structural transitions of DNA driven by external torques and forces [38]. There is no evidence of base extrusion since the amplitude of ϕ is largely confined to a value of 0.4 rad. Results presented in Figs. 5–7 correspond to the following optimization scheme: $K_{\mathrm{sa}}=2\times10^4$, $T_{\mathrm{i}}=5.0\times10^7$,$T_{\mathrm{f}}=5.0\times10^2$, and $\alpha_{\mathrm{sa}}=0.05$. Velocity of the soliton v can be obtained by fitting Eq. (12) to the time series of $\chi(t)$. This gives us a dimensionless value of 2.66×10^{-4}. Despite the resemblance, one feature remains missing, that is, the increase in contour length as a result of the untwisting of the helix and unstacking of the bases [39]. This arises from the neglect of the coupling between ϕ and r in Eq. (3). To see the effects of this coupling, we can simply replace ϵ with $[(\epsilon-\epsilon')/4][\cos(\phi_{\mathrm{n+1}}-\phi_{\mathrm{n}})+\cos(\phi'_{\mathrm{n+1}}-\phi'_{\mathrm{n}})]+(\epsilon+\epsilon')/2$ so that when the bases are extruded from the double helix, the barrier between B-DNA and S-DNA is removed. Effects of this modification can be seen in Fig. 8. A more stable stretched intermediate is produced as evident in

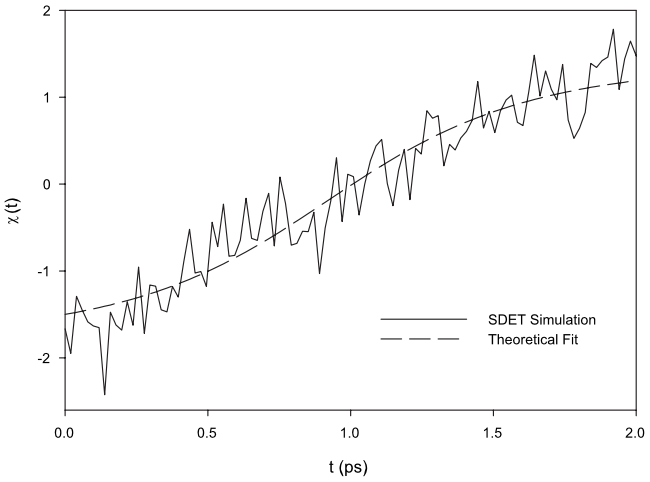

FIG. 5. Plot of $\chi(z=\xi-\xi_0-vT)$. Equation (12) is fitted to the simulation results to determine the soliton velocity.

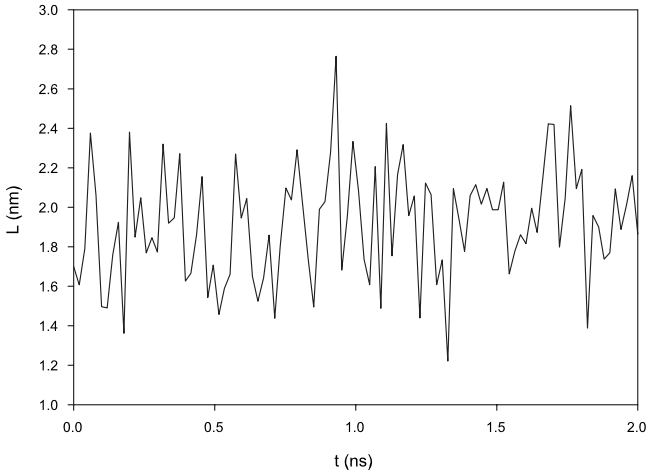

FIG. 6. The oligomer stretches to a maximum value of 2.76 nm during the transition, which corresponds to a relative extension of 1.63, a value that is consistent with the relative extension of the intermediate found in atomistic simulations.

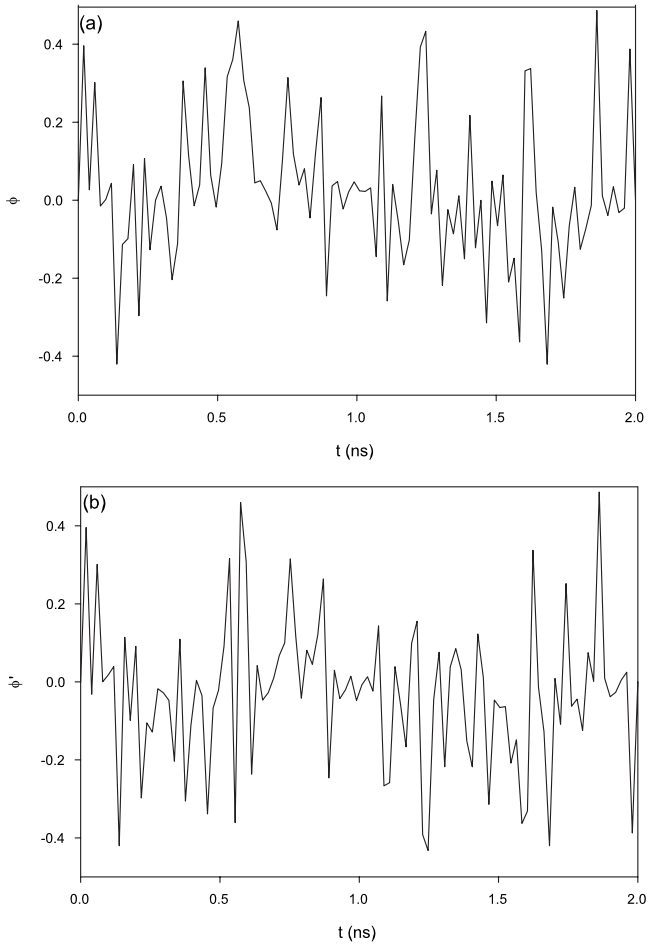

FIG. 7. Time series of (a) ϕ and (b) ϕ' for an arbitrary nucleobase. Results are taken from a DNA oligomer with $N=6$. $\phi(t)$ fluctuates about a mean value of 2.69×10^{-2}, which is small enough to be consistent with the assumption used in our derivation of the Harvey model.

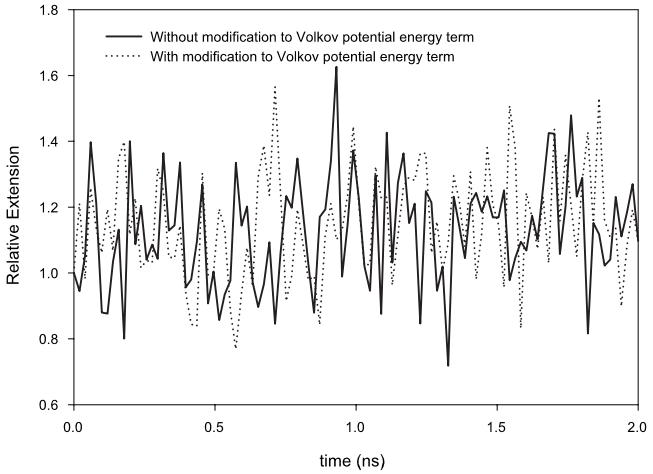

FIG. 8. With the modification to ϵ, the stretched intermediate is more stable as shown by the decrease in the fluctuation amplitude.

the reduced fluctuation and the increase in the average relative extension of the intermediate structures. Note also that the modification has no bearing on the analytical results of the Harvey-zipper model.

We can also investigate the variation in relative extension of the oligomer with length (or equivalently, the number of base pairs). At this juncture, one faces a problem with determining the total time needed to simulate B-Z DNA transition. It is not immediately obvious how T_{tot} varies with length. This is due to contradicting experimental data which does not clearly indicate whether the rate constant of the transition increases or decreases with the length of the oligomer [10]. Consequently, several simulations with different T_{total}'s are run with at least 1.3 million annealing steps. The results, presented in Fig. 9, are nonetheless consistent despite the choice of T_{total}. An increase in polymer length leads to a decrease in relative extension for the intermediate structures. For a shorter strand, it is easier for the DNA to overcome the stacking interaction between base pairs and stretches in order to remove any steric constraint during base flipping. However, as the length increases, the possibility of stretching the entire strand decreases due to the increase in total stacking energy. Note also that the amplitude of ϕ oscillation for individual nucleobase remains unchanged with the length of the strand as indicated in Fig. 10. However, if the ensemble average of ϕ oscillation $\langle\phi\rangle_N$ is taken, then one observes from Fig. 11 that the amplitude of $\langle\phi\rangle_N$ decreases with increasing length due to the increase in total stacking interaction that has to be overcome for base extrusion. We expect the results to be slightly modified when the coupling between r and ϕ is taken into account. This will be done in future studies.

VII. CONCLUSION

In summary, for a sufficiently long DNA strand where base extrusion angle is time-averaged to be zero, i.e., $\langle\phi\rangle=0$, and longitudinal displacement about the equilibrium point y is small, one can expect the transition to follow the

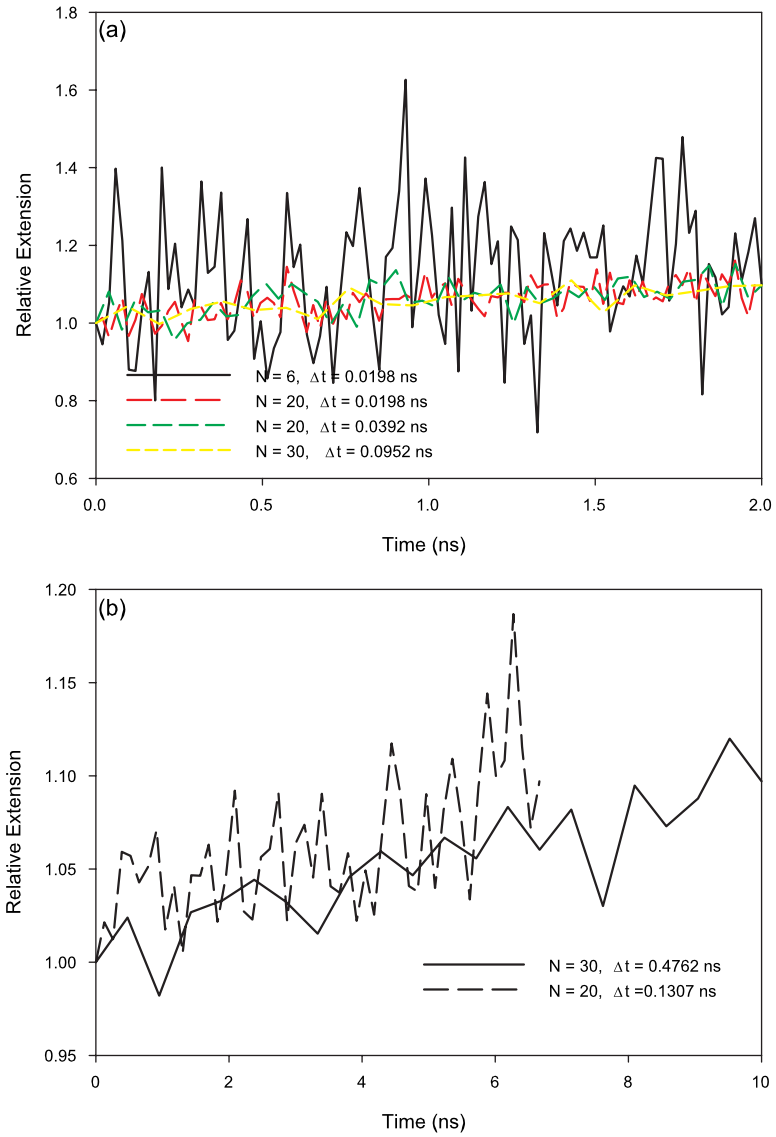

FIG. 9. (Color online) Time series of relative extension. (a) Total time of simulation is 2.0 ns. As the size of the oligomer increases, the relative extension of the intermediate structures decreases. (b) Conclusion remains the same despite the increase in simulation time.

Harvey-zipper model. If $r_n > b$ and $N \gg 1$, then the Zang-Olson or Wang mechanism is more likely to take place. Finally, in the limit of small N, the transition will occur via means of a stretched intermediate. In light of these possibilities, one must reassess the experimental investigations on B-Z DNA transition [40–44]. The size of the DNA strand used in the studies may actually affect base pair opening probabilities which in turn can influence proton exchange in NMR studies. The dynamics of a GC segment contained within or attached to a much longer λ-DNA strand is different from an equivalent independent segment. Use of intercalating agents, negative supercoiling and B-Z inducers to facilitate B-Z DNA transition can also influence the manner in which the transition proceeds. For instance, negative supercoiling unwinds and stretches the strand to give rise to the condition $r_n > b$, resulting in helix opening. Substitution such as cytosine methylation can also affect the values of b and I and destabilizes the helix. Finally, salt-induced experiments can influence the value of λ as a result of electrostatic screening.

A mean field approach adopted here can also prove useful in studying specific conformational transitions in large DNA

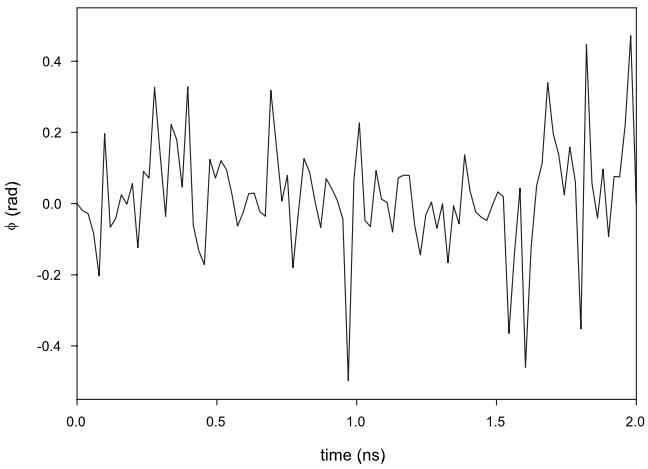

FIG. 10. Time series of ϕ for an oligomer with $N=20$. Comparing this figure with Fig. 7, the amplitude of ϕ oscillation is approximately the same, taking a maximum value of 0.47 rad. $\langle\phi\rangle$ on the other hand equals 2.12×10^{-2} rad, a value that remains close to zero and is smaller than the corresponding value in Fig. 7 by 20%.

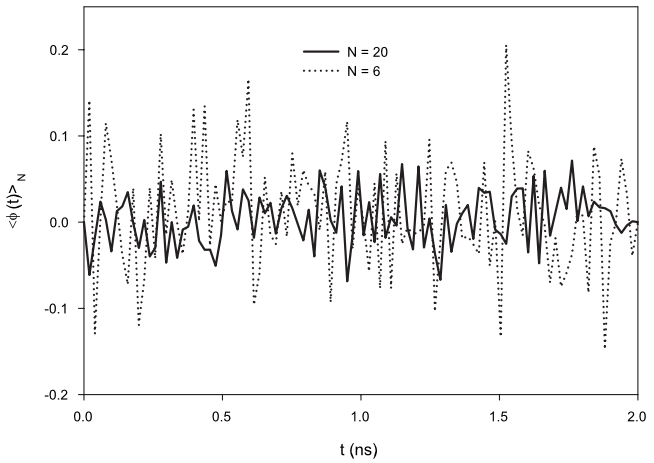

FIG. 11. Time series of ensemble average $\langle\phi\rangle_N$ for both $N=20$ and $N=6$. Amplitude of $\langle\phi\rangle_N$ oscillation for $N=6$ is larger, taking a maximum value of 0.21 rad as compared to 0.071 rad for $N=20$.

strands since atomistic simulations are computationally expensive [5]. Despite the slow rate of convergence with the simulated annealing schemes, the numerical solutions derived here using the SDET algorithm are still able to paint a qualitatively accurate dynamical picture of the transition. Future studies using more elaborate DNA models may include the helicoidal structure of DNA [45,46], the dynamics of sugar-pucker rings during the transition and its interaction with the nucleobases. This is, however, done at the expense of computational time and simplicity.

The statistical mechanics of B-Z DNA transition can also be investigated in the current framework [23,47,48]. Using the soliton gas model in the Harvey-zipper model, the number density n of χ solitons in the helix is given by $(4\sqrt{2AK}/pi)K_1(4\sqrt{2AK}/k_BT)$ where K_n is the modified Bessel function of the second kind and $4\sqrt{2AK}$ is the "mass" of a χ soliton. Using this result, one may be able to obtain an estimate of the rate constant $R \approx N_z/N = n\Delta z$, where Δz is the length of a B-Z junction. At low temperatures $k_BT \ll 4\sqrt{2AK}$, we have $\ln R = \ln(\Delta z/\sqrt{\pi}) + \frac{1}{2}\ln(4\sqrt{2AKk_BT}) - 4\sqrt{2AK}\ln(e)/k_BT$. Comparison between the theoretical results presented here and experimental data can provide us with some estimates on the length of the B-Z junction and the mass of a χ soliton. Note however that the independent soliton gas model has to be treated with caution in the Zang-Olson model as a result of the interaction between ϕ and χ solitons [8]. More investigation, both experimental and theoretical, can be done in this area.

[1] S. W. Englander, N. R. Kallenbach, A. J. Heeger, J. A. Krumhansl, and S. Litwin, Proc. Natl. Acad. Sci. U.S.A. **77**, 7222 (1980).
[2] S. Yomosa, Phys. Rev. A **30**, 474 (1984).
[3] C.-T. Zhang, Phys. Rev. A **35**, 886 (1987).
[4] L. V. Yakushevich, Int. J. Quantum Chem. **88**, 570 (2002).
[5] L. V. Yakushevich, J. Biosci. **26**, 305 (2001).
[6] T. Dauxois, M. Peyrard, and A. R. Bishop, Phys. Rev. E **47**, R44 (1993).
[7] M. Salerno, Phys. Rev. A **44**, 5292 (1991).
[8] L. V. Yakushevich, A. V. Savin, and L. I. Manevitch, Phys. Rev. E **66**, 016614 (2002).
[9] V. Muto, P. S. Lomdahl, and P. L. Christiansen, Phys. Rev. A **42**, 7452 (1990).
[10] M. A. Fuertes, V. Cepeda, C. Alonso, and J. M. Pérez, Chem. Rev. (Washington, D.C.) **106**, 2045 (2006).
[11] K. L. Sung Chul Ha, A. Rich, Y.-G. Kim, and K. K. Kim, Nature (London) **437**, 1183 (2005).
[12] A. T. Ansevin and A. H. Wang, Nucleic Acids Res. **18**, 6119 (1990).
[13] W. Saenger and U. Heinermann, FEBS Lett. **257**, 223 (1989).
[14] S. C. Harvey, Nucleic Acids Res. **11**, 4867 (1983).
[15] A. H. Wang, G. J. Quigley, F. J. Kolpak, J. L. Crawford, J. H. van Boom, G. van der Marel, and A. Rich, Nature (London) **282**, 680 (1979).
[16] P. Jensen, M. V. Jarić, and K. H. Bennemann, Phys. Lett. **95A**, 204 (1983).
[17] Z. Zang and W. Olson, *A Model for the B-Z Transition of DNA involving Solitary Excitations*, Series in Solid State Vol. 69 (Springer-Verlag, New York, 1987), p. 265.
[18] W. Lim and Y. P. Feng, Biophys. J. **88**, 1593 (2005).
[19] W. Lim and Y. P. Feng, Biopolymers **78**, 107 (2004).
[20] W. Lim and Y. P. Feng, Biophys. Rev. Lett. **1**, 279 (2006).
[21] M. A. Kastenholz, T. U. Schwartz, and P. H. Hnenberger, Biophys. J. **91**, 2976 (2006).
[22] S. N. Volkov, J. Theor. Biol. **143**, 485 (1990).
[23] L. V. Yakushevich, *Nonlinear Physics of DNA* (John Wiley & Sons Ltd., Chichester, 1998).
[24] S. Cocco and R. Monasson, Phys. Rev. Lett. **83**, 5178 (1999).
[25] D. Hennig and J. F. R. Archilla, Physica A **331**, 579 (2004).
[26] N. Foloppe and J. Alexander D. MacKerell, J. Phys. Chem. B **103**, 10955 (1999).
[27] N. Foloppe, B. Hartmann, L. Nilsson, J. Alexander D. MacKerell, Biophys. J. **82**, 1554 (2002).
[28] J. Šponer, H. A. Gabb, J. Leszczynski, and P. Hobza, Biophys. J. **73**, 76 (1997).
[29] J. Šponer, H. A. Gabb, J. Leszczynski, and P. Hobza, Biophys. J. **73**, 76 (1997).
[30] Zhou Haijun, Zhang Yang, and Ou-Yang Zhong-can, Phys. Rev. Lett. **82**, 4560 (1999).
[31] H. Zhou, Y. Zhang, and Z. Ou-Yang, Phys. Rev. E **62**, 1045 (2000).
[32] J. F. Allemand, D. B. R. Lavery, and V. Croquette, Proc. Natl. Acad. Sci. U.S.A. **95**, 14152 (1998).
[33] M. Elstner, P. Hobza, T. Frauenheim, S. Suhai, and E. Kaxiras, J. Chem. Phys. **114**, 5149 (2001).
[34] J. Mazur, R. L. Jernigan, and A. Sarai, Mol. Biol. **37**, 240 (2003).
[35] M. F. Guasti, Physica D **189**, 188 (2004).
[36] J. F. Léger, G. Romano, A. Sarkar, J. Robert, L. Bourdieu, D. Chatenay, and J. F. Marko, Phys. Rev. Lett. **83**, 1066 (1999).
[37] R. Elber, A. Cárdenas, A. Ghosh, and H. A. Stern, Adv. Chem.

Phys. **126**, 93 (2003).
[38] A. Sarkar, J.-F. Léger, D. Chatenay, and J. F. Marko, Phys. Rev. E **63**, 051903 (2001).
[39] P.-Y. Lai and Z.-C. Zhou, Chin. J. Phys. (Taipei) **40**, 465 (2002).
[40] S. Sen and R. Majumdar, Nucleic Acids Res. **15**, 5863 (1987).
[41] R. D. Sheardy, N. Levine, S. Marotta, D. Suh, and J. B. Chaires, Biochemistry **33**, 1385 (1994).
[42] H. Zhang, H. Yu, J. Ren, and X. Qu, Biophys. J. **90**, 3203 (2006).
[43] F. Aboul-ela, R. P. Bowater, and D. M. J. Lilley, J. Biol. Chem. **267**, 1776 (1992).
[44] J. Markovits, J. Ramstein, B. P. Roques, and J.-B. L. Pecq, Nucleic Acids Res. **13**, 3773 (1985).
[45] T. Dauxois, Phys. Lett. A **159**, 390 (1991).
[46] G. Gaeta, Phys. Lett. A **172**, 365 (1993).
[47] L. V. Yakushevich, *Methods of Theoretical Physics and Their Applications to Biopolymer Science* (Nova Science Publishers, Commack, 1996).
[48] J. F. Currie, J. A. Krumhansl, A. R. Bishop, and S. E. Trullinger, Phys. Rev. B **22**, 477 (1980).
[49] It has been pointed out that certain parameters such as K_n should include the covalent bonding energy in the sugar phosphate chain so as to ensure a more stable solution. In view of the fact that the current analysis has neglected sugar-phosphate dynamics, such considerations can be made in future investigations.